Appl Biochem Biotechnol (2013) 169:1566–1578
DOI 10.1007/s12010-012-0078-x

# Bovine Serum Albumin Nanospheres Synchronously Encapsulating "Gold Selenium/Gold" Nanoparticles and Photosensitizer for High-Efficiency Cancer Phototherapy

**Cong Yu · Fangjie Wo · Yuxiang Shao · Xiangyun Dai · Maoquan Chu**

Received: 3 October 2012 / Accepted: 27 December 2012 /
Published online: 16 January 2013
© Springer Science+Business Media New York 2013

**Abstract** Gold nanostructures have generated significant attention in biomedical areas because of their major role in cancer photothermal therapeutics. In order to conveniently combine gold nanostructures and drugs into one nanocomposite, $Au_2Se$/Au core–shell nanostructures with strong near-infrared-absorbing properties were synthesized using a simple method and embedded inside bovine serum albumin (BSA) nanospheres by using a spray dryer equipped with an ultrasonic atomizer followed by thermal denaturation. The nanospheres with narrow size distribution mainly ranging from 450 to 600 nm were obtained. The $Au_2Se$/Au-loaded BSA nanospheres (1 mg) adsorbed at least 0.01 mg of water-insoluble zinc phthalocyanine (ZnPc) photosensitizer. After irradiation with a 655-nm laser (20 min), the temperature of the $Au_2Se$/Au-loaded BSA nanospheres [200 μL, 2 mg/mL, BSA/$Au_2Se$/Au 10:1 (*w*/*w*)] increased by over 20 °C from the initial temperature of 24.82±0.15 °C, and the release of ZnPc was improved compared with a corresponding sample without irradiation. After being incubated with cancer cells (human esophageal carcinoma Eca-109), the nanospheres exhibited photothermal and photodynamic therapy with a synergistic effect upon laser irradiation. This work provides novel $Au_2Se$/Au-loaded polymer nanospheres prepared by a high-efficiency strategy for incorporating drugs for improving the efficiency in killing cancer cells.

**Keywords** $Au_2Se$/Au core–shell nanoparticles · BSA nanospheres · ZnPc photosensitizer · Light-triggered drug release · Combinational therapy

Cong Yu, Fangjie Wo, and Yuxiang Shao contributed equally to this work.

C. Yu · F. Wo · Y. Shao · X. Dai · M. Chu
School of Life Science and Technology, Tongji University, Shanghai 200092, People's Republic of China

M. Chu (✉)
Suzhou Institute of Tongji University, Suzhou, People's Republic of China
e-mail: mqchu98@tongji.edu.cn

## Introduction

Compared with normal tissue, tumor tissue has poor blood supply and a slow blood stream flow, which cause the poor heat dissipation effect in tumors. Therefore, it has been demonstrated that tumors could be destroyed at temperatures over 42.5 °C [1], whereas, normal tissue could survive at temperatures up to 44 °C [2]. In order to selectively heat tumors and to avoid damaging the surrounding normal tissue, tumors are injected with photothermal agents and then heated by photothermal conversion induced by laser irradiation. This photothermal conversion has attracted much attention during the past few decades. The photothermal conversion efficiency is controlled by the kind of photothermal agents used if the laser power is remained constant. Up to now, gold nanostructures (e.g., nanoshells [3–8], nanocages [9, 10], nanorods [11, 12], and nanocubes [13]), carbon-based nanoparticles [14–21], quantum dots [22], and indocyanine green [23–25] have been used for cancer photothermal therapy. However, the disadvantage with indocyanine green molecules is their photobleaching under laser irradiation. Compared with the carbon-based nanomaterials and quantum dots, gold nanostructures exhibit a strong absorption in the near-infrared (NIR) region due to their strong NIR surface plasmon resonance. In addition, the gold nanostructures are easy to synthesize, and their optical properties can be controlled conveniently by varying the particle morphology and size [26–28]. Therefore, recently, more attention has been given to gold nanostructures for cancer photothermal therapy [3–13, 26–30].

However, the efficiency of the cancer therapy using photothermal treatment alone is limited. Combining methods of treatment is a more promising efficient strategy for eradicating cancer. For example, photothermal therapy using gold nanostructures combined with chemotherapy or photodynamic therapy appears to be a more aggressive approach compared to any individual method of treatment as described above [31–35]. The main formation methods of the gold–anticancer drug complexes are as follows: drugs are dispersed inside gold shell-coated polymer (or liposome) nanospheres [7, 32]; drugs are adsorbed onto polyethylene glycol-modified gold nanorods by charge–charge interaction [33]; and drugs are incorporated into hollow gold nanospheres [34] or gold nanocages [35]. Among the above drug–gold complexes, gold shell-coated polymer spheres may be suitable for carrying a large amount of drugs because of the large and adjustable volume of the polymer spheres. It is known that gold is a heavy metal; therefore, the biocompatibility of gold nanoparticles embedded inside polymer spheres may be better than that of the gold shell-coated polymer spheres because the gold material is protected by the polymer spheres in the former structure.

In this paper, gold nanoparticles with an interior composed of gold selenium (gold selenium/gold core–shell particles), having strong NIR-absorbing properties, were synthesized. We then used a highly efficient spray-drying strategy to incorporate such core–shell gold nanostructures into bovine serum albumin (BSA) nanospheres. A photosensitizer drug [zinc phthalocyanine (ZnPc)] was incorporated into the gold-loaded BSA nanospheres. The drug-loaded nanospheres obtained synchronously exhibited photothermal and photodynamic effects upon laser irradiation, which has great potential for cancer phototherapy (Fig. 1).

## Materials and Methods

### Materials

Gold chloride tetrahydrate ($HAuCl_4$) and ZnPc were purchased from Sigma-Aldrich (St. Louis, MO, USA). BSA powder was purchased from the Shi Cheng Biotechnology

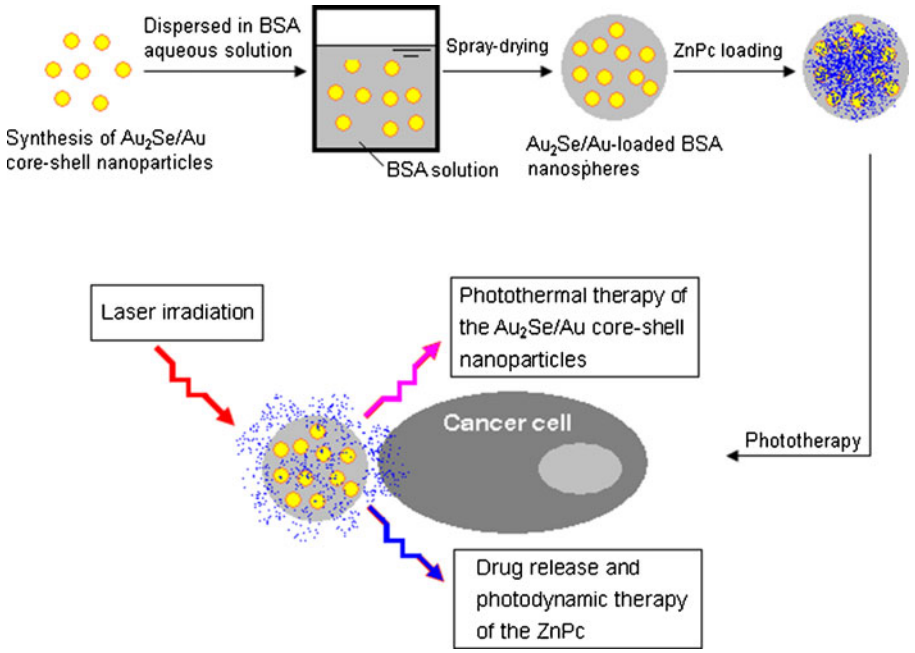


**Fig. 1** Schematic of the formation of a ($Au_2Se$/Au and ZnPc)-loaded BSA nanospheres for cancer phototherapy

Company (Shanghai, China). $NaSeSO_4$, dimethyl sulfoxide (DMSO), $HNO_3$, $HClO_4$, and distilled water were purchased from Sinopharm Chemical Reagent Co., Ltd. (Shanghai, China). Human esophageal carcinoma cells (Eca-109) were ordered from the Chinese Academy of Sciences (Shanghai, China). RPMI-1640 culture medium and fetal calf serum (FCS) were obtained from Gibco (Carlsbad, CA, USA). Double stain apoptosis detection kit [Hoechst 33342/propidium iodide (PI)] was purchased from Sigma-Aldrich. CellTiter-Glo® Luminescent Cell Viability Assay reagents were purchased from Promega Corporation (Madison, WI, USA).

## Synthesis of $Au_2Se$/Au Core–Shell Nanoparticles

$HAuCl_4$ (3 mM) and $NaSeSO_4$ (2 mM) aqueous solutions (the volume ratio of $NaSeSO_4$ to $HAuCl_4$ was 1:10) were mixed together and stirred at room temperature, and the solution absorption spectrum was monitored every 15 min using a UV/Vis spectrophotometer (UV-2102PC, Unico). After the absorption peak shifted to an NIR wavelength, the reaction solution was precipitated via centrifugation and washed two times with distilled water to remove the free Au colloids.

## Preparation of $Au_2Se$/Au-Loaded BSA Nanospheres

A spray dryer equipped with an ultrasonic atomizer (Jiangyin Spray Dryer Factory, China) was used for preparing the nanospheres. For a typical experiment, 0.25 g of BSA powder was dissolved in 25 mL of distilled water, and the $Au_2Se$/Au nanoparticles were then dispersed in the BSA solution. The mass ratios of BSA to $Au_2Se$/Au were set at 50:1,

50:3, and 50:5, respectively. The inlet temperature was set at 100 °C, and the feed flow rate was about 20 mL/h. The powders obtained were then heated to 150 °C and then maintained at this temperature for 3 h.

## Incorporation of ZnPc Photosensitizer and ZnPc Content Measurement

$Au_2Se$/Au-loaded BSA nanosphere powder (2 mg) was added into 4 mL of saturated ZnPc ethanol solution [containing 50 % (*v*/*v*) of DMSO] and stirred in a dark room overnight. After then, the solution was precipitated via centrifugation and washed with ethanol to remove the free ZnPc.

For detecting the ZnPc content in the nanospheres, 1 mL of the ($Au_2Se$/Au and ZnPc)-loaded BSA nanospheres (2 mg/mL) aqueous solution was treated with 5 mL of $HNO_3$ at 100 °C for 2 h and 1 mL of $HClO_4$ at 120 °C until it was no longer visibly cloudy. $HNO_3$ (5 mL) was added into the sample again. About 30 min later, the sample was diluted with distilled water for detecting the Zn atoms in the solution using inductively coupled plasma–atomic emission spectrometry (ICP-AES) (iCAP6300, Thermo Jarrell Ash Co., Franklin, MA, USA).

## Characterization

The morphology of the $Au_2Se$/Au core–shell nanoparticles was investigated using a high-resolution transmission electron microscope (HRTEM) (JEOL 2010) equipped with an X-ray spectroscopy [energy-dispersive spectroscopy (EDS)] (Oxford) analysis system, operating at 200 kV. The morphologies of the $Au_2Se$/Au-loaded BSA nanospheres were observed using a scanning electron microscope (SEM) (JSM-6360LV, JEOL). The size distributions of the BSA nanospheres were analyzed through the SEM results with about 200 particles for each sample. UV-Vis absorption spectra were recorded on the diode array spectrophotometer.

## Photothermal Conversion

For evaluating the photothermal conversion of the $Au_2Se$/Au-loaded BSA nanospheres, 200 μL of water-dispersed nanospheres (2 mg/mL) was placed in small glass tubes and irradiated for 0–20 min using a laser with the wavelength of 655 nm (power density: 0.5 W/cm$^2$; spot area, 5×8 mm; Shanghai Inter-Diff Optoelectronics Tech Co., Ltd., Shanghai, China). The original temperature of the solutions was maintained at 24.82±0.15 °C, and the temperature increase was detected using a chromel–alumel thermocouple thermometer (Shanghai Instrument Factory Co., Ltd., Shanghai, China) equipped with an induction probe.

## In Vitro Drug Release Experiments

$Au_2Se$/Au-loaded BSA nanospheres (3 mg) was added into 6 mL of saturated ZnPc ethanol/DMSO [1:1 (*v*/*v*)] solution and stirred in a dark room for 12 h. The mixture solution was equally divided into six parts, three served as the experiment groups and the remaining three parts served as the control groups. After centrifugation and washing with ethanol to remove the free ZnPc, each sample was redispersed into 300 μL of ethanol/DMSO solution in a small plastic centrifugal tube at room temperature. The experiment groups were irradiated using the 655-nm laser for 20 min in a dark room, and the control groups were placed in a dark room for 20 min without laser irradiation. After then, the suspensions of the samples were centrifuged immediately, and the absorption intensities of the supernatant solutions were measured at a wavelength of 670 nm.

### Cell Experiments

Human esophageal carcinoma Eca-109 cells were seeded into 96-well plates and cultured in 100 μL of RPMI-1640 medium containing 10 % FCS and 1 % penicillin/streptomycin (Gibco) in an incubation chamber (37 °C, 5 % $CO_2$). To observe the interaction between the cancer cells and ($Au_2Se$/Au and ZnPc)-loaded BSA nanospheres, the culture medium was removed, and the culture media (without FCS)-dispersed nanospheres (200 μg/mL) were added to the cells and incubated with the cells at 37 °C. Two hours later, the cells were washed more than five times with PBS and imaged using a fluorescent microscope (Leica DME, Germany).

To evaluate cell viability, the cells were divided into two groups: one with laser irradiation and one without. Each group was respectively incubated with culture medium-dispersed $Au_2Se$/Au-loaded BSA nanospheres and ($Au_2Se$/Au and ZnPc)-loaded BSA nanospheres. The concentration of the $Au_2Se$/Au-loaded BSA nanospheres was 333 μg/mL, and the concentration of ZnPc in the nanospheres was 3.3 μg/mL. After incubation for 2 h, the irradiation groups were irradiated with the 655-nm laser in a dark room for 20 min. One hour later, the culture medium was removed, and the Hoechst 33342/PI double staining reagents (propidium iodide, 10 μg/mL; Hoechst 33342, 3 μg/mL) were added to the above cells and incubated for 20 min. For the non-irradiation groups, the cells were cultured for the same time as above and then also added with the double staining reagents. The cell fluorescence (EX=488 nm) was then assessed using a fluorescent microscope (Leica DME, Wetzlar, Germany).

In order to quantitatively measure the number of esophageal carcinoma Eca-109 cells that survived before and after irradiation, the cell viability was measured with the CellTiter-Glo® Luminescent Cell Viability Assay. The cells were also divided into laser and non-laser groups. Each group was respectively incubated with culture medium-dispersed $Au_2Se$/Au-loaded BSA nanospheres, ($Au_2Se$/Au and ZnPc)-loaded BSA nanospheres and ZnPc. The concentrations of the nanospheres and ZnPc were the same as described above. After incubation for 2 h, the irradiation groups were irradiated with the 655-nm laser for 20 min. One hour later, the CellTiter-Glo reagent (100 μL) was added into each well and mixed for 10 min, and the cell viability of each group was then measured by its luminescence using the Flexstation III enzyme-labeled instrument (Molecular Devices, Sunnyvale, CA). For the groups without irradiation, the cell viabilities were measured using the same methods as described above. As controls, the viabilities of the cells containing only the culture medium with and without irradiation were measured.

## Results and Discussion

The gold nanoparticles encapsulated in BSA nanospheres in this work are core-shell composite structures ($Au_2Se$/Au) (Fig. 2a). The synthesis process of those core–shell nanostructures is simple and highly efficient. The HRTEM image showed that the shell thickness was about 3 nm, and the average diameter of the cores was about 24 nm. The $Au_2Se$/Au core–shell nanoparticles were washed two times with water; therefore, most of the free gold nanoparticles in the samples may have been removed, which could be demonstrated by the absorption spectra (Fig. 2b). As shown in Fig. 2b, the absorption peak at about 525 nm comes from the free gold nanoparticles [36], and the absorption peak between 600 and 1,000 nm comes from the gold nanoshells. The peak intensity at about 525 nm significantly decreased, and the peak intensity between 600 and 1,000 nm obviously increased with

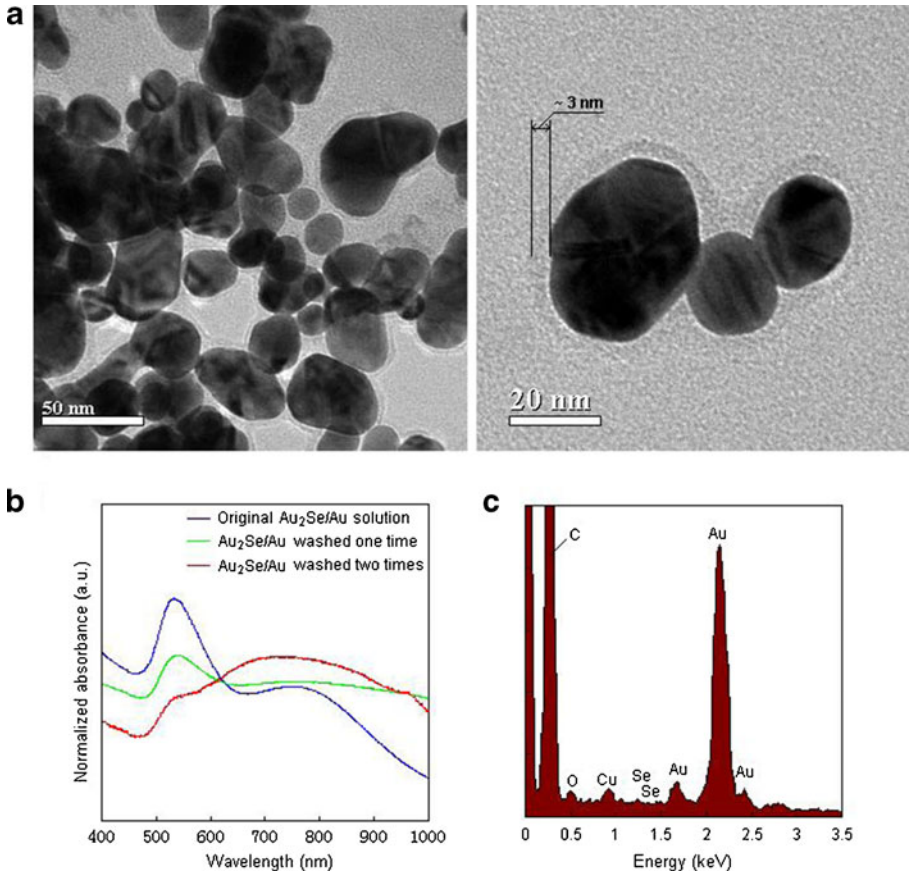


**Fig. 2** Characterization of $Au_2Se$/Au core–shell nanoparticles. **a** HRTEM images of the $Au_2Se$/Au nanoparticles washed two times (*left* small magnification; *right* larger magnification). **b** Absorption spectra of the $Au_2Se$/Au nanoparticles before and after washing with water. **c** EDS of the $Au_2Se$/Au nanoparticles washed two times

increasing washing times, which indicates that the purification of the sample could be performed by a simple washing process. The strong NIR absorption of the $Au_2Se$/Au nanoparticles is interesting because these nanoparticles may exhibit high photothermal conversion efficiency after being irradiated by a NIR light. EDS detection showed that the gold nanoparticles are mainly composed of elemental Au and Se (O, Cu, and C derived from the ambient air and a copper mesh) (Fig. 2c), which further demonstrated the high purity of the washed $Au_2Se$/Au nanoparticles.

However, bare $Au_2Se$/Au nanoparticles do not adsorb a sufficient amount of drugs easily. For loading drugs, $Au_2Se$/Au nanoparticles were encapsulated into BSA nanospheres using a spray-drying method. Because the diameter of the aqueous droplets produced by the ultrasonic atomizer ranges mainly from the sub-micrometer to only several micrometers, which is significantly smaller than the droplets produced by the rotary atomizer (five to several hundred micrometers), we selected a spray dryer equipped with an ultrasonic atomizer for the preparation of the $Au_2Se$/Au-loaded BSA nanospheres in the present work. The SEM images show that the BSA nanospheres obtained with or without $Au_2Se$/Au

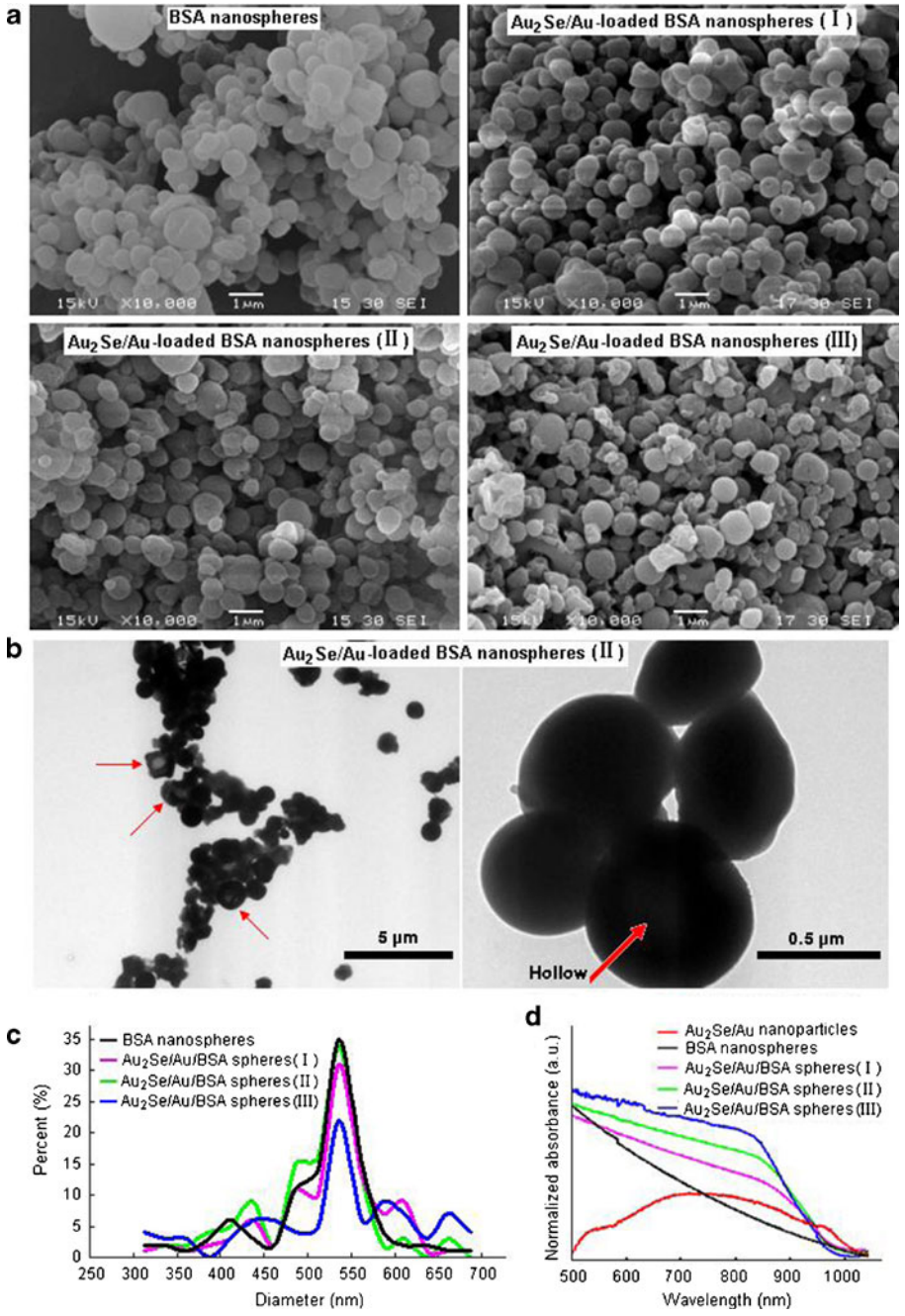


**Fig. 3** Morphologies, size distributions, and absorption spectra of BSA and $Au_2Se$/Au-loaded BSA nanospheres incorporated with different amounts of $Au_2Se$/Au nanoparticles. **a** SEM images and **b** TEM images (*left* low magnification; *right* high magnification). **c** Size distributions. **d** Absorption spectra (including $Au_2Se$/Au). The samples I, II, and III denote that the mass ratios of BSA to $Au_2Se$/Au in the nanospheres were 50:1, 50:3, and 50:5, respectively

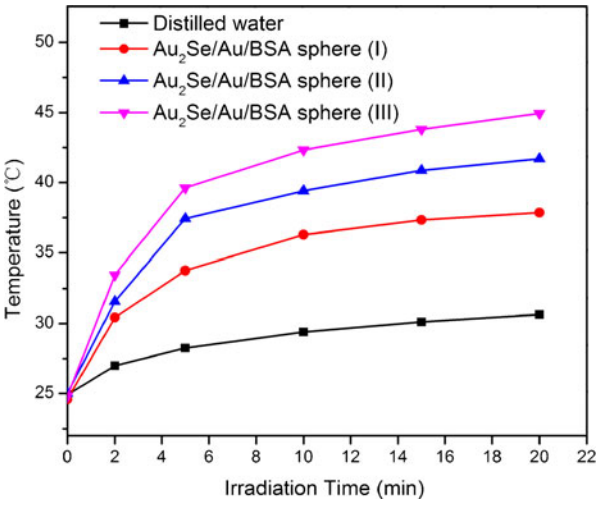


**Fig. 4** Temperature increase of the distilled water and water-dispersed $Au_2Se$/Au-loaded BSA nanospheres upon irradiation with a 655-nm laser. All samples were 200 μL in volume and contained 2 mg/mL of $Au_2Se$/Au-loaded BSA nanospheres (except distilled water). The samples I, II, and III denote that the mass ratios of BSA to $Au_2Se$/Au in the nanospheres were 50:1, 50:3, and 50:5, respectively

exhibit a narrower size distribution ranging mainly from 450 to 600 nm (Fig. 3a). A small amount of the nanospheres have hollow structures, but most of the nanospheres are solid, as confirmed by the TEM images (Fig. 3b). The number of larger nanospheres slightly increases with increasing amounts of $Au_2Se$/Au core–shell nanoparticles (from 0.2 mg/mL through 0.6 to 1 mg/mL) in the spray-dry precursors (Fig. 3c).

The $Au_2Se$/Au-loaded BSA nanospheres retained the NIR-absorbing properties of the $Au_2Se$/Au nanoparticles. The more $Au_2Se$/Au nanoparticles are incorporated in the BSA nanospheres, the higher was the absorption intensity ranging from 600 to 900 nm (Fig. 3d). Therefore, the $Au_2Se$/Au-loaded BSA nanospheres may have a high photothermal conversion efficiency. As shown in Fig. 4, with a 655-nm laser irradiation, the temperature of the water-dispersed $Au_2Se$/Au-loaded BSA nanospheres rapidly increased from the initial temperature of 24.82±0.15 °C in a short time. With increasing amounts of $Au_2Se$/Au nanoparticles embedded in the BSA nanospheres, the temperatures of the $Au_2Se$/Au-loaded BSA nanospheres increased after irradiation. For example, when the mass ratios of BSA to

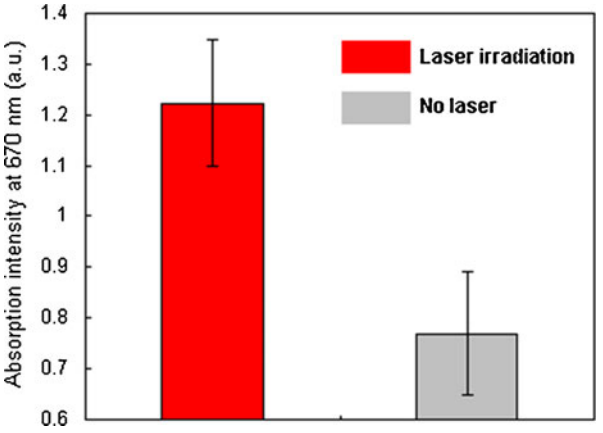


**Fig. 5** Drug release monitored by the absorption intensities at a 670-nm wavelength of the supernatant solutions obtained from the ($Au_2Se$/Au and ZnPc)-loaded BSA nanospheres with and without 655-nm laser irradiation. The mass ratio of BSA to $Au_2Se$/Au in the nanospheres was 50:3

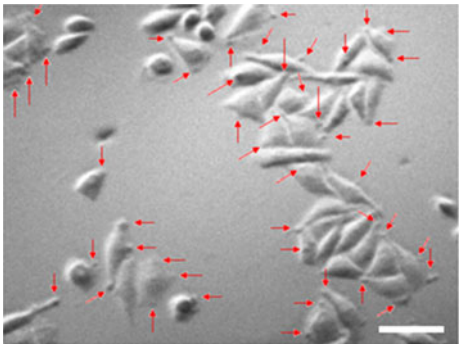

**Fig. 6** Bright field image of the esophagus carcinoma cells incubated with ($Au_2Se$/Au and ZnPc)-loaded BSA nanospheres. The mass ratio of BSA to $Au_2Se$/Au in the nanospheres was 50:3. *Scale bar* 20 μm

$Au_2Se$/Au nanoparticles were 50:1, 50:3, and 50:5, the temperature of 200 μL of the nanospheres (2 mg/mL) increased over 13.26, 16.70, and 20.15 °C, respectively, after irradiation for 20 min, whereas the temperature of 200 μL of distilled water increases only over 5.74 °C after irradiation for 20 min. This indicates that the temperature increase is mainly due to the photothermal conversion of the $Au_2Se$/Au-loaded BSA nanospheres.

In order to improve the cancer therapy efficiency, a photosensitizer, ZnPc, was incorporated into the $Au_2Se$/Au-loaded BSA nanospheres through free diffusion. ICP-AES analysis shows that 1 mg of the nanospheres could load at least 0.01 mg of ZnPc. After 300 μL of the

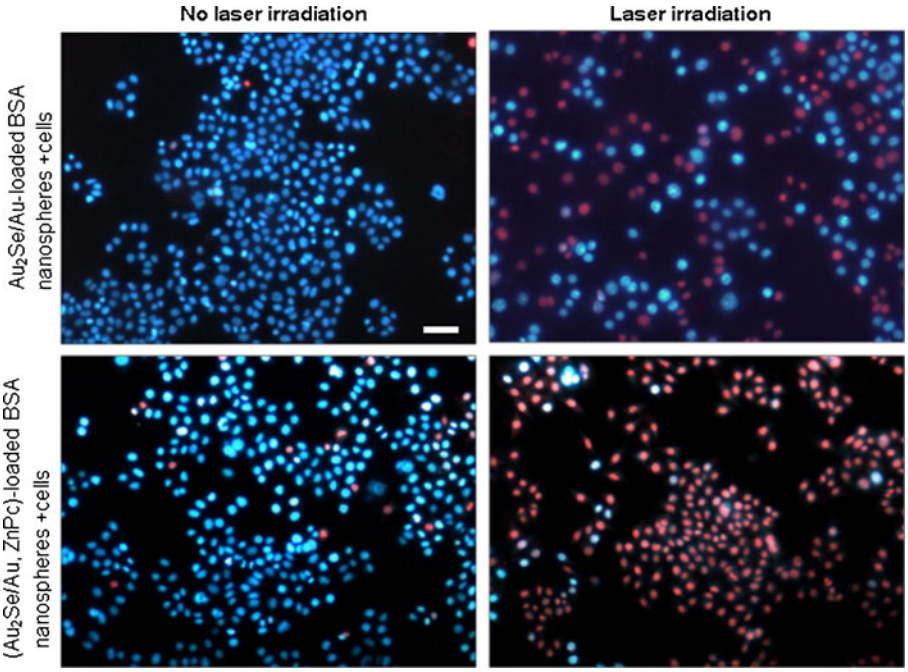


**Fig. 7** Fluorescence images of the esophagus carcinoma cells incubated with $Au_2Se$/Au-loaded BSA nanospheres and ($Au_2Se$/Au and ZnPc)-loaded BSA nanospheres with and without 655-nm laser irradiation. The mass ratio of BSA to $Au_2Se$/Au in the nanospheres was 50:3. Scale bar: 50 μm

($Au_2Se$/Au and ZnPc)-loaded BSA nanospheres [1.69 mg/mL, BSA:$Au_2Se$/Au=50:3 (wt/wt)] were irradiated using the 655-nm laser for 20 min, and the resulting suspensions were centrifuged, the average absorption peak intensity (at 670-nm wavelength) of the supernatant solutions was 1.60 times as much as that of the supernatant solutions obtained from the ($Au_2Se$/Au and ZnPc)-loaded BSA nanospheres without laser irradiation (Fig. 5). This indicates that the release of ZnPc from the ($Au_2Se$/Au and ZnPc)-loaded BSA nanospheres is more rapid than that without irradiation, which may be due to the increased speed of molecular thermodynamic movement at higher temperature. More ZnPc release is beneficial for photodynamic therapy when the ($Au_2Se$/Au and ZnPc)-loaded BSA nanospheres are incubated with cancer cells.

When the esophagus carcinoma cells (Eca-109) were incubated with ($Au_2Se$/Au and ZnPc)-loaded BSA nanospheres [200 μg/mL, BSA/$Au_2Se$/Au=50:3 (*w*/*w*), ZnPc=2 μg/mL] at 37 °C for 2 h and then washed with PBS more than five times; most of the cells were still decorated with the nanospheres (Fig. 6, see arrows). The ability of cancer cells to firmly adsorb the nanospheres is a benefit for the following phototherapy because the cells can easily receive the heat and drug released from the nanospheres.

We used the Hoechst 33342/PI double staining reagents for analysis of the viability of the cancer cells treated with the BSA nanospheres and laser irradiation. As shown in Fig. 7, when the esophagus carcinoma cells were incubated with the $Au_2Se$/Au-loaded BSA nanospheres [333 μg/mL, BSA/$Au_2Se$/Au=50:3 (*w*/*w*)] without laser irradiation, nearly all the cells emitted blue fluorescence, which indicated that $Au_2Se$/Au-loaded BSA nanospheres

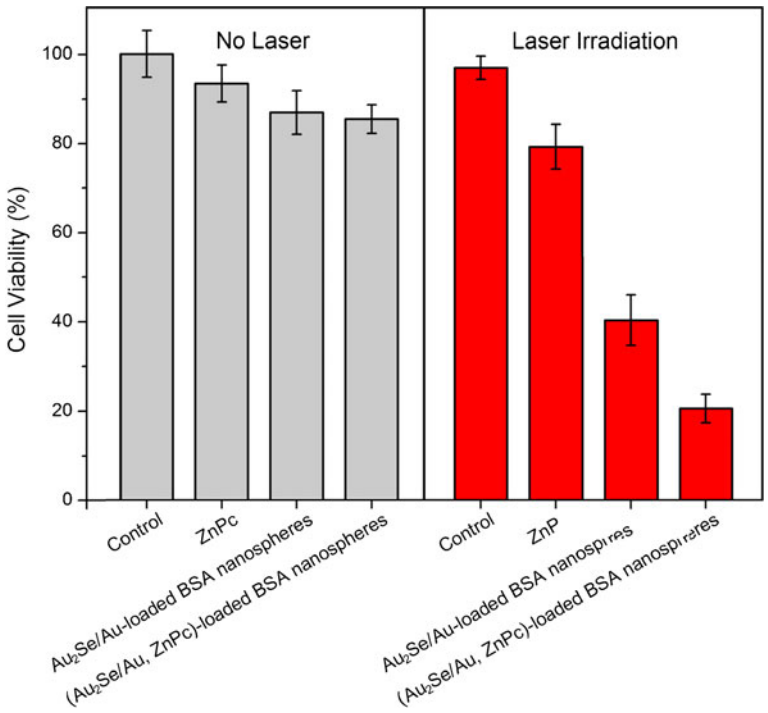


**Fig. 8** Esophagus carcinoma cell viability after the cells were incubated with ZnPc, $Au_2Se$/Au-loaded BSA nanospheres, and ($Au_2Se$/Au and ZnPc)-loaded BSA nanospheres with and without 655-nm laser irradiation and controls. The mass ratio of BSA to $Au_2Se$/Au in the nanospheres was 50:3

nearly had no toxicity to cells. After the ZnPc drug being incorporated into those nanospheres and then being incubated with the cancer cells without laser irradiation, small amount of the cells may die since small amount of the cells emitted red fluorescence. It is known that ZnPc is a highly effective photosensitizer. Once the cells incubated with the nanospheres were exposed to the outside light (e.g., sunlight lamp) during the cell experimental operation, the ZnPc would generate phototoxicity. It is surprised that most of the cells may be killed when the cells were respectively incubated with the above two nanospheres upon 20 min of laser irradiation, and the phototherapy efficiency of the ($Au_2Se$/Au and ZnPc)-loaded BSA nanospheres was higher than that of the $Au_2Se$/Au-loaded BSA nanospheres.

The efficiency of the above nanospheres killing esophagus carcinoma cells was further analyzed using a luminescent assay by a CellTiter-Glo reagent based on the quantitation of ATP present in the cells. As shown in Fig. 8, when the ($Au_2Se$/Au and ZnPc)-loaded BSA nanospheres [333 μg/mL, BSA/$Au_2Se$/Au=50:3 (*w*/*w*), ZnPc=3.33 μg/mL] were incubated with the cancer cells and subsequently irradiated using the 655-nm laser for 20 min, only about 20.55±3.22 % of the cells survived. When the nanospheres with the same concentration as above, but without ZnPc, were incubated with the cancer cells, about 40.28±5.70 % of the cells survived after irradiation for 20 min, and 79.23±4.19 % of the cells survived when the cells were incubated with ZnPc alone (3.3 μg/mL) after 20 min of irradiation. ZnPc is a water-insoluble photosensitizer, so its aqueous suspension phototoxicity toward cells is not high. For the groups incubated with the $Au_2Se$/Au-loaded nanospheres or ZnPc alone without irradiation, however, the cell viability was obviously higher (85–94 %) than those with irradiation, and laser irradiation alone did not obviously effect the cell viability. The results described above indicated that the ($Au_2Se$/Au and ZnPc)-loaded BSA nanospheres exhibited excellent $Au_2Se$/Au nanostructure photothermal therapy and ZnPc photodynamic therapy with a synergistic effect.

In summary, BSA nanospheres synchronously incorporated with $Au_2Se$/Au core–shell nanostructures and ZnPc photosensitizer have been successfully developed through a highly efficient spray-drying technique using a spray dryer equipped with an ultrasonic atomizer. Cancer cells combinational treatment through photothermal therapy of $Au_2Se$/Au nanostructures and photodynamic therapy of ZnPc were conveniently carried out, induced by only a beam of light generated by a laser. We believe that the proposed $Au_2Se$/Au-loaded BSA nanospheres may be as a platform for incorporating various drugs for high-efficiency combinational therapy in the future.

**Acknowledgments** This work was supported in part by the National Natural Science Foundation of China (81071833), the Natural Science Foundation of Jiangsu Province (SBK201123093), and the Program for New Century Excellent Talents in University (NCET-07-0618).

## References

1. Raaphorst, G. P. (1990). Fundamental aspects of hyperthermic biology. In S. B. Field & J. W. Hand (Eds.), *An introduction to the practical aspects of clinical hyperthermia* (pp. 10–54). London: Taylor & Francis.
2. Fajardo, L. F. (1984). Pathological effects of hyperthermia in normal tissues. *Cancer Research, 44*, 4826s–4835s.
3. Hirsch, L. R., Stafford, R. J., Bankson, J. A., Sershen, S. R., Rivera, B., Price, R. E., et al. (2003). Nanoshell-mediated near-infrared thermal therapy of tumors under magnetic resonance guidance. *Proceedings of the National Academy of Sciences of the United States of America, 100*, 13549–13554.
4. Lowery, A. R., Gobin, A. M., Day, E. S., Halas, N. J., & West, J. L. (2006). Immunonanoshells for targeted photothermal ablation of tumor cell. *International Journal of Nanomedicine, 1*, 149–154.

5. Gobin, A. M., Lee, M. H., Halas, N. J., James, W. D., Drezek, R. A., & West, J. L. (2007). Near-infrared resonant nanoshells for combined optical imaging and photothermal cancer therapy. *Nano Letters, 7*, 1929–1934.
6. Stern, J. M., Stanfield, J., Kabbani, W., Hsieh, J. T., & Cadeddu, J. A. (2008). Selective prostate cancer thermal ablation with laser activated gold nanoshells. *Journal of Urology, 179*, 748–753.
7. Park, H., Yang, J., Lee, J., Haam, S., Choi, I. H., & Yoo, K. H. (2009). Multifunctional nanoparticles for combined doxorubicin and photothermal treatments. *ACS Nano, 3*, 2919–2926.
8. Wu, C. Y., Yu, C., & Chu, M. Q. (2011). A gold nanoshell with a silica inner shell synthesized using liposome templates for doxorubicin loading and near-infrared photothermal therapy. *International Journal of Nanomedicine, 6*, 807–813.
9. Chen, J., Wang, D., Xi, J., Au, L., Siekkinen, A., Warsen, A., et al. (2007). Immuno gold nanocages with tailored optical properties for targeted photothermal destruction of cancer cells. *Nano Letters, 7*, 1318–1322.
10. Skrabalak, S. E., Au, L., Lu, X., Li, X., & Xia, Y. (2007). Gold nanocages for cancer detection and treatment. *Nanomedicine, 2*, 657–668.
11. Hauck, T. S., Jennings, T. L., Yatsenko, T., Kumaradas, J. C., & Chan, W. C. W. (2008). Enhancing the toxicity of cancer chemotherapeutics with gold nanorod hyperthermia. *Advanced Materials, 20*, 3832–3838.
12. Huang, X. H., El-Sayed, I. H., Qian, W., & El-Sayed, M. A. (2006). Cancer cell imaging and photothermal therapy in the near-infrared region by using gold nanorods. *Journal of the American Chemical Society, 128*, 2115–2120.
13. Wu, X., Ming, T., Wang, X., Wang, P. N., Wang, J. F., & Chen, J. Y. (2010). High-photoluminescence-yield gold nanocubes: for cell imaging and photothermal therapy. *ACS Nano, 4*, 113–120.
14. Liu, X. W., Tao, H. Q., Yang, K., Zhang, S. A., Lee, S. T., & Liu, Z. A. (2011). Optimization of surface chemistry on single-walled carbon nanotubes for in vivo photothermal ablation of tumors. *Biomaterials, 32*, 144–151.
15. Markovic, Z. M., Harhaji-Trajkovic, L. M., Todorovic-Markovic, B. M., Kepic, D. P., Arsikin, K. M., Jovanovic, S. P., et al. (2011). In vitro comparison of the photothermal anticancer activity of graphene nanoparticles and carbon nanotubes. *Biomaterials, 32*, 1121–1129.
16. Huang, N. Y., Wang, H. Q., Zhao, J. H., Lui, H., Korbelik, M., & Zeng, H. S. (2010). Single-wall carbon nanotubes assisted photothermal cancer therapy: animal study with a murine model of squamous cell carcinoma. *Lasers in Surgery and Medicine, 42*, 638–648.
17. Burke, A., Ding, X. F., Singh, R., Kraft, R. A., Levi-Polyachenko, N., Rylander, M. N., et al. (2009). Long-term survival following a single treatment of kidney tumors with multiwalled carbon nanotubes and near-infrared radiation. *Proceedings of the National Academy of Sciences of the United States of America, 106*, 12897–12902.
18. Chakravarty, P., Marches, R., Zimmerman, N. S., Swafford, A. D., Bajaj, P., Musselman, I. H., et al. (2008). Thermal ablation of tumor cells with antibody-functionalized single-walled carbon nanotubes. *Proceedings of the National Academy of Sciences of the United States of America, 105*, 8697–8702.
19. Zhang, M. F., Murakami, T., Ajima, K., Tsuchida, K., Sandanayaka, A. S., Ito, O., et al. (2008). Fabrication of ZnPc/protein nanohorns for double photodynamic and hyperthermic cancer phototherapy. *Proceedings of the National Academy of Sciences of the United States of America, 105, 14773–14778.*
20. Yang, K., Zhang, S., Zhang, G., Sun, X., Lee, S. T., & Liu, Z. (2010). Graphene in mice: ultrahigh in vivo tumor uptake and efficient photothermal therapy. *Nano Letters, 10*, 3318–3323.
21. Chu, M., Peng, P., Zhao, J., Liang, S., Shao, Y., & Wu, Q. (2013). Laser light triggered-activated carbon nanosystem for cancer therapy. *Biomaterials, 34*, 1820–1832.
22. Chu, M., Pan, X., Zhang, D., Wu, Q., Peng, J., & Hai, W. (2012). The therapeutic efficacy of CdTe and CdSe quantum dots for photothermal cancer therapy. *Biomaterials, 33*, 7071–7083.
23. Abels, C., Karrer, S., BaumLer, W., Goetz, A. E., Landthaler, M., & Szeimies, R. M. (1998). Indocyanine green and laser light for the treatment of AIDS-associated cutaneous Kaposi's sarcoma. *British Journal of Cancer, 77*, 1021–1024.
24. Zheng, X., Xing, D., Zhou, F., Wu, B., & Chen, W. R. (2011). Indocyanine green-containing nanostructure as near infrared dual-functional targeting probes for optical imaging and photothermal therapy. *Molecular Pharmaceutics, 8*, 447–456.
25. Lim, H. J., & Oh, C. H. (2011). Indocyanine green-based photodynamic therapy with 785 nm light emitting diode for oral squamous cancer cells. *Photodiagnosis and Photodynamic, 8*, 337–342.
26. Huang, X. H., Jain, P. K., El-Sayed, I. H., & El-Sayed, M. A. (2008). Plasmonic photothermal therapy (PPTT) using gold nanoparticles. *Lasers in Medical Science, 23*, 217–228.
27. Huang, X. H., & El-Sayed, M. A. (2010). Gold nanoparticles: optical properties and implementations in cancer diagnosis and photothermal therapy. *Journal of Advanced Research, 1*, 13–28.

28. Jelveh, S., & Chithrani, D. B. (2011). Gold nanostructures as a platform for combinational therapy in future cancer therapeutics. *Cancers, 3*, 1081–1110.
29. Day, E. S., Bickford, L. R., Slater, J. H., Riggall, N. S., Drezek, R. A., & West, J. L. (2010). Antibody-conjugated gold-gold sulfide nanoparticles as multifunctional agents for imaging and therapy of breast cancer. *International Journal of Nanomedicine, 5*, 445–454.
30. Gobin, A. M., Watkins, E. M., Quevedo, E., Colvin, V. L., & West, J. L. (2010). Near-infrared-resonant gold/gold sulfide nanoparticles as a photothermal cancer therapeutic agent. *Small, 6*, 745–752.
31. Jin, H., Hong, B., Kakar, S. S., & Kang, K. A. (2008). Tumor-specific nano-entities for optical detection and hyperthermic treatment of breast cancer. *Advances in Experimental Medicine and Biology, 614*, 275–284.
32. Paddock, C. (2010). Gold-coated liposomes could make chemo more effective, less harmful. Available from: www.mednewstoday.com. Accessed October 1, 2011.
33. Jang, B., Park, J. Y., Tung, C. H., Kim, I. H., & Choi, Y. (2011). Gold nanorod-photosensitizer complex for near-infrared fluorescence imaging and photodynamic/photothermal therapy in vivo. *ACS Nano, 5*, 1086–1094.
34. You, J., Zhang, G. D., & Li, C. (2010). Exceptionally high payload of doxorubicin in hollow gold nanospheres for near-infrared light-triggered drug release. *ACS Nano, 4*, 1033–1041.
35. Yavuz, M. S., Cheng, Y. Y., Chen, J. Y., Cobley, C. M., Zhang, Q., Rycenga, M., et al. (2009). Gold nanocages covered by smart polymers for controlled release with near-infrared light. *Nature Materials, 8*, 935–939.
36. Norman, T. J., Grant, C. D., Magana, D., Zhang, J. Z., Liu, J., Cao, D. L., et al. (2002). Near infrared optical absorption of gold nanoparticle aggregates. *The Journal of Physical Chemistry. B, 106*, 7005–7012.